

ORBITAL PRECESSION FROM THE ECE2 LAGRANGIAN

by

M. W. Evans and H. Eckardt,

Civil List and AIAS / UPITEC

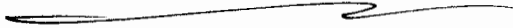
(www.aias.us, www.upitec.org, www.archive.org, www.webarchive.org, www.et3m.net)

ABSTRACT

Orbital precession is shown to be the result of ECE2 relativity and the relevant lagrangian, both in two dimensional and three dimensional orbits. For example, precession of the perihelion of Mercury can be produced by this theory. Einsteinian general relativity is not only incorrect but irrelevant. The same type of lagrangian analysis is applied to find novel equations of quantum mechanics.

Keywords: ECE2 relativity, orbital precession from the lagrangian, lagrangian quantum mechanics.

UFT 372



1. INTRODUCTION

In recent papers of this series {1 - 12}, ECE2 lagrangian theory has been applied to the dynamics of gyroscopes, three dimensional orbits and a novel lagrangian quantum mechanics. In Section 2 it is shown that the lagrangian of ECE2 special relativity leads to orbital precession without use of the incorrect and obsolete Einsteinian general relativity. ECE2 relativity has been developed in UFT313 ff. on combined sites www.aias.us and www.upitec.org. It has the structure of special relativity, but is developed in a space with non zero torsion and curvature. Therefore the ECE2 lagrangian is the lagrangian of special relativity. The relevant Euler Lagrange equations can be solved simultaneously with the same numerical methods as used in UFT368 to UFT371. This solution leads directly to a precessing orbit which can be compared with astronomical data as in Section 3. The same lagrangian methods lead to novel results of general utility in quantum mechanics. These new equations of quantum mechanics are summarized in Section 2.

This paper is a brief synopsis of extensive calculations found in the accompanying notes for UFT372 on www.aias.us. Note 372(1) gives the basic equations of the new lagrangian approach, exemplified by the H atom. The latter is described in terms of a quantized plane elliptical orbit. Note 372(2) discusses the $l = 0$ state of the hydrogen atom, and Note 372(3) sets up the hamiltonian for the helium atom. Notes 372(4) and 372(5) give details of the calculation of the relativistic orbit and notes 372(6) to 372(8) develop new general equations of quantum mechanics from the lagrangian method.

Section 3 gives graphical results for the precessing orbit, and makes a comparison with the astronomical data for the precession of the perihelion of planets in the solar system. It also discusses Moebius orbits.

2. PRECESSING ORBITS AND LAGRANGIAN QUANTUM MECHANICS

Consider the lagrangian of ECE2 relativity {1 - 12}:

$$\mathcal{L} = -mc^2 \left(1 - \frac{v^2}{c^2}\right)^{1/2} + \frac{mMG}{r} \quad - (1)$$

in which a mass m orbits a mass M in a plane defined by the plane polar coordinates

(r, ϕ) . The magnitude of the distance between m and M is r , and the orbital velocity

of m is:

$$v^2 = \dot{r}^2 + r^2 \dot{\phi}^2 \quad - (2)$$

Here c is the speed of light in vacuo. The proper Lagrange variables are r and ϕ , and

the Euler Lagrange equations are:

$$\frac{\partial \mathcal{L}}{\partial r} = \frac{d}{dt} \frac{\partial \mathcal{L}}{\partial \dot{r}} \quad - (3)$$

and

$$\frac{\partial \mathcal{L}}{\partial \phi} = \frac{d}{dt} \frac{\partial \mathcal{L}}{\partial \dot{\phi}} \quad - (4)$$

These are solved simultaneously to give:

$$\frac{dr}{d\phi} = \frac{\dot{r}}{\dot{\phi}} \quad - (5)$$

and the orbit

$$r = \int \frac{dr}{d\phi} d\phi \quad - (6)$$

Q. E. D. The numerical method uses Runge Kutta integration with Maxima as described in

UFT368 to UFT371. The orbit is a precessing ellipse, Q. E. D., and is graphed in Section 3.

A precessing ellipse is therefore produced by ECE2 relativity, there is no need for the obsolete and incorrect Einstein theory.

The three dimensional lagrangian is the same as Eq. (1), but:

$$v^2 = \dot{r}^2 + r^2 \dot{\beta}^2 \quad - (7)$$

where

$$\dot{\beta}^2 = \dot{\theta}^2 + \dot{\phi}^2 \sin^2 \theta \quad - (8)$$

in the spherical polar coordinates system (r, θ, ϕ) . The proper Lagrange variables are r , θ , and ϕ , and the three Euler Lagrange equations are:

$$\frac{\partial \mathcal{L}}{\partial r} = \frac{d}{dt} \frac{\partial \mathcal{L}}{\partial \dot{r}} \quad - (9)$$

$$\frac{\partial \mathcal{L}}{\partial \theta} = \frac{d}{dt} \frac{\partial \mathcal{L}}{\partial \dot{\theta}} \quad - (10)$$

$$\frac{\partial \mathcal{L}}{\partial \phi} = \frac{d}{dt} \frac{\partial \mathcal{L}}{\partial \dot{\phi}} \quad - (11)$$

These are solved simultaneously in Section 3 and again give a precessing orbit, the details of which are graphed in Section 3. In this case the precessing planar orbit can be tilted with respect to orbit given by plane polar coordinates. In certain circumstances this can give rise to astronomically observable Moebius strip orbits as graphed in Section 3.

In theory, this orbital Lagrange theory can be applied to the quantization of the hydrogen (H) atom by using the Coulomb potential:

$$U = -\frac{e^2}{4\pi\epsilon_0 r} \quad - (12)$$

in the lagrangian (1). Here e is the charge on the proton, and ϵ_0 the vacuum permittivity. The classical velocity of the electron in the H atom is:

$$\underline{v} = \dot{r} \underline{e}_r + r \dot{\theta} \underline{e}_\theta + r \dot{\phi} \sin\theta \underline{e}_\phi \quad - (13)$$

in spherical polar coordinates, with unit vectors \underline{e}_r , \underline{e}_θ , and \underline{e}_ϕ .

Quantization takes place as follows:

$$i\hbar \frac{\partial \psi}{\partial t} = E \psi \quad - (14)$$

$$-i\hbar \underline{\nabla} \psi = \underline{p} \psi \quad - (15)$$

where the gradient of the wavefunction is:

$$\underline{\nabla} \psi = \frac{\partial \psi}{\partial r} \underline{e}_r + \frac{1}{r} \frac{\partial \psi}{\partial \theta} \underline{e}_\theta + \frac{1}{r \sin\theta} \frac{\partial \psi}{\partial \phi} \underline{e}_\phi. \quad - (16)$$

Not that the relativistic energy:

$$E = \gamma mc^2 \quad - (17)$$

and momentum:

$$\underline{p} = \gamma m \underline{v} \quad - (18)$$

are used in the quantization.

The first order quantum equations are therefore:

$$i\hbar \frac{\partial \psi}{\partial t} = E \psi = \gamma mc^2 \psi = \left(1 - \frac{v^2}{c^2}\right)^{-1/2} mc^2 \psi \quad - (19)$$

$$-i\hbar \frac{\partial \psi}{\partial r} = \gamma m r \dot{\psi} \quad - (20)$$

$$-i\hbar \frac{\partial \psi}{\partial \theta} = \gamma m r^2 \dot{\theta} \psi \quad - (21)$$

$$-i\hbar \frac{\partial \psi}{\partial \phi} = \gamma m r^2 \sin^2 \theta \dot{\phi} \psi \quad - (22)$$

There is also the second order equation:

$$-\hbar^2 \nabla^2 \psi = p^2 \psi = \gamma^2 m^2 v^2 \psi \quad - (23)$$

In the non relativistic limit these equations become:

$$i\hbar \frac{\partial \psi}{\partial t} = E \psi \quad - (24)$$

$$-i\hbar \frac{\partial \psi}{\partial r} = m r \dot{\psi} \quad - (25)$$

$$-i\hbar \frac{\partial \psi}{\partial \theta} = m r^2 \dot{\theta} \psi \quad - (26)$$

$$-i\hbar \frac{\partial \psi}{\partial \phi} = m r^2 \sin^2 \theta \dot{\phi} \psi \quad - (27)$$

and:

$$-\hbar^2 \nabla^2 \psi = m^2 v^2 \psi \quad - (28)$$

In preceding UFT papers and in UFT270, the lagrangian method was used on the classical level to give the classical angular momenta:

$$L^2 = m^2 r^4 (\dot{\theta}^2 + \dot{\phi}^2 \sin^2 \theta) \quad - (29)$$

and

$$L_z = m r^2 \dot{\phi} \sin^2 \theta. \quad - (30)$$

It is well known {1 - 12} that these quantize as follows for all atoms and molecules:

$$\hat{L}^2 \psi = \hbar^2 l(l+1) \psi \quad - (31)$$

$$\hat{L}_z \psi = \hbar m_l \psi \quad - (32)$$

where l is the angular momentum quantum number and where:

$$m_l = -l, \dots, l \quad - (33)$$

is the azimuthal quantum number.

By quantum classical equivalence

$$\hat{L}_z \psi = \hbar m_l \psi = m r^2 \sin^2 \theta \dot{\phi} \psi \quad - (34)$$

giving the expectation value of Lagrangian quantum mechanics:

$$\langle m r^2 \dot{\phi} \sin^2 \theta \rangle = \hbar m_l. \quad - (35)$$

Similarly:

$$\langle m^2 r^4 (\dot{\theta}^2 + \dot{\phi}^2 \sin^2 \theta) \rangle = l(l+1) \hbar^2 \quad - (36)$$

so

$$\langle m r^2 \dot{\theta} \rangle = \frac{\hbar}{2} (\ell(\ell+1) - m_e^2) \quad - (37)$$

From Lagrangian theory on the classical level:

$$m r^2 \dot{\theta} = \left(\frac{L^2 - L_z^2}{\sin^2 \theta} \right)^{1/2} \quad - (38)$$

giving the expectation value:

$$\left\langle \frac{L^2 - L_z^2}{\sin^2 \theta} \right\rangle = \hbar^2 (\ell(\ell+1) - m_e^2) \quad - (39)$$

of Lagrangian quantum mechanics.

In summary, the expectation values are:

$$\int \psi^* m r^2 \dot{\theta} \psi d\tau = \frac{\hbar}{2} (\ell(\ell+1) - m_e^2)^{1/2} \quad - (40)$$

$$\int \psi^* m r^2 \dot{\phi} \sin^2 \theta \psi d\tau = \hbar m_e \quad - (41)$$

$$\int \psi^* \sin^2 \theta \psi d\tau = L_z^2 \left(L^2 - \hbar^2 (\ell(\ell+1) - m_e^2) \right)^{-1} \quad - (42)$$

From Eqs. (26) and (40):

$$-i \int \psi^* \frac{\partial \psi}{\partial \theta} d\tau = (\ell(\ell+1) - m_e^2)^{1/2} \quad - (43)$$

From Eqs. (27) and (41):

$$-i \int \psi^* \frac{\partial \psi}{\partial \phi} d\tau = m_e \quad - (44)$$

From Eqs. (27) and (39):

$$L^2 - \frac{L_z^2}{\sin^2 \theta} = -i\hbar^2 \int \psi^* \frac{\partial \psi}{\partial \theta} d\tau \quad (45)$$

These are fundamental equations of Lagrangian quantum mechanics.

3. COMPUTATIONAL AND GRAPHICAL RESULTS

Section by Dr. Horst Eckardt

Orbital precession from the ECE2 Lagrangian

M. W. Evans*, H. Eckardt†
Civil List, A.I.A.S. and UPITEC

(www.webarchive.org.uk, www.aias.us,
www.atomicprecision.com, www.upitec.org)

3 Computational and graphical results

3.1 Relativistic Lagrange equations

The relativistic Euler-Lagrange equations (9-11) in three dimensions, based on the Lagrange function (1), have been worked out by computer and solved numerically as described in previous papers. Spherical polar coordinates (r, θ, ϕ) are used. By re-inserting the terms $\gamma = 1/\sqrt{1 - v^2/c^2}$ and v from Eq. (7) they take the form:

$$\ddot{\theta} = -\frac{(2\gamma c^2 r - GM) \dot{r} \dot{\theta} - \gamma c^2 \dot{\phi}^2 r^2 \cos(\theta) \sin(\theta)}{\gamma c^2 r^2}, \quad (46)$$

$$\ddot{\phi} = -\frac{\dot{\phi} \left(2\gamma c^2 r^2 \cos(\theta) \dot{\theta} + (2\gamma c^2 r - GM) \dot{r} \sin(\theta) \right)}{\gamma c^2 r^2 \sin(\theta)}, \quad (47)$$

$$\ddot{r} = -\frac{(\gamma c^2 r - GM) \dot{r}^2 - \gamma v^2 c^2 r + GM c^2}{\gamma c^2 r^2}. \quad (48)$$

By the transition $c \rightarrow \infty$, one obtains the non-relativistic form:

$$\ddot{\theta} = \dot{\phi}^2 \cos(\theta) \sin(\theta) - \frac{2\dot{r} \dot{\theta}}{r}, \quad (49)$$

$$\ddot{\phi} = -\frac{2\dot{\phi} \cos(\theta) \dot{\theta}}{\sin(\theta)} - \frac{2\dot{\phi} \dot{r}}{r}, \quad (50)$$

$$\ddot{r} = r \dot{\theta}^2 + \dot{\phi}^2 r \sin^2(\theta) - \frac{GM}{r^2}. \quad (51)$$

For planar orbits it is sufficient to write the equations in two dimensions. This corresponds to omitting the polar angle θ :

$$\ddot{\phi} = -\frac{(2\gamma c^2 r - GM) \dot{r} \dot{\phi}}{\gamma c^2 r^2}, \quad (52)$$

$$\ddot{r} = -\frac{(\gamma c^2 r - GM) \dot{r}^2 - \gamma v^2 c^2 r + GM c^2}{\gamma c^2 r^2}. \quad (53)$$

*email: emyrone@aol.com

†email: mail@horst-eckardt.de

Again, the non-realistic transition can be made, resulting in the well-known form

$$\ddot{\phi} = -\frac{2\dot{r}\dot{\phi}}{r}, \quad (54)$$

$$\ddot{r} = r\dot{\phi}^2 - \frac{GM}{r^2}. \quad (55)$$

It is possible to rewrite Eqs. (52, 53) further. With the abbreviation

$$r_0 = \frac{2MG}{c^2} \quad (56)$$

(Schwarzschild radius) they take the form

$$\ddot{\phi} = \left(\frac{r_0}{2\gamma r} - 2 \right) \frac{\dot{r}\dot{\phi}}{r}, \quad (57)$$

$$\ddot{r} = r\dot{\phi}^2 + \frac{r_0}{2\gamma r^2}\dot{r}^2 - \frac{GM}{\gamma r^2} = r\dot{\phi}^2 + \frac{1}{2}r_0(\dot{r}^2 - c^2)\frac{1}{\gamma r^2}. \quad (58)$$

It is seen that this is identical with the non-relativistic form, augmented by one term of order $1/c^2$ each (represented by r_0). Since the product $\dot{r}\dot{\phi}$ takes both signs around the perihelion, we have a symmetric modification of angular acceleration in this region. The gravitational potential is modified by the γ factor but more important is the additional term introducing a dependence on \dot{r} which was not there in the non-relativistic case. From the right-most form of Eq. (58) we see that the potential is counteracted by \dot{r} . In the ultrarelativistic case the potential is nearly without effect.

The solutions of Eqs. (46-48) are graphed in Fig. 1. This is a gravitational planetary system with model parameters chosen so that relativistic effects are visible. The motion stays planar even in the relativistic case. The radial oscillations of the periodic orbit can be seen. The orbit looks regular, however inspection by the orbit plot (Fig. 2) shows that it is a precessing ellipse. The plane of motion is tilted against the XY plane by the initial conditions of $\dot{\theta}$. The graph of angular momenta L and L_Z (Fig. 3) shows that these are no more constants of motion in this relativistic case. The γ factor is graphed in Fig. 4. It shows peaks at the perihelion where orbital velocity is much higher than at aphelion. This variation demonstrates that we have a solution of general relativity.

3.2 Perihelion precession of Mercury

One of the few experimental confirmations of Einstein's theory of general relativity was the explanation of perihelion precession of planet Mercury. This is a tiny effect, and influences of other planets on the Mercury precession are much larger than the part explained by Einstein. This was extensively discussed in UFT 239. In UFT 322 we mentioned that the observed precession of the perihelion is $7.9673 \cdot 10^{-7}$ radians per year. Since Mercury has an orbital period of 88.0 days, the precession angle per one revolution is

$$\Delta\phi = 7.9673 \cdot 10^{-7} \cdot \frac{88.0}{365.25} \text{rad} = 1.9196 \cdot 10^{-7} \text{rad}. \quad (59)$$

This is a very small value, therefore a calculation of orbital time evolution has to be highly precise. We cannot do this without considerable numerical effort. As an alternative, we propose an interpolation scheme where the orbit is calculated by artificially increased relativistic effects, $\Delta\phi$ is determined from the orbit and then an extrapolation is made to the real value of the relativistic parameters. The Schwarzschild radius r_0 could be used for this in Eqs. (57, 58). Then the algorithm is:

- Compute $\Delta\phi(r_1)$ where r_1 is an increased r_0
- repeat for several values r_2, r_3, \dots for building up a function $\Delta\phi(r_i)$
- extrapolate function $\Delta\phi(r_i)$ for value $r = r_0$

By this algorithm the numerical precision can be checked simultaneously.

3.3 Moebius orbit

In cosmology some extraordinary structures like a Moebius strip can be observed. This strip structure has been tried to reproduce by a simple calculation. We used two masses orbiting a common centre in tilted orbits. The two masses are independent, i.e. there is the assumption that the interaction between orbiting masses is small compared to the gravity of the centre. This seems reasonable. The initial condition for ϕ of the second mass has been shifted slightly so that both orbits have no common points. Fig. 5 shows the orbits, in Fig. 6 the difference vector between both masses has been plotted. This shows the structure of a Moebius strip. It is assumed that there are much more than two masses moving in the 2D area between the two plotted orbits.

This is a quite simple and classical explanation of the observed Moebius structure. In cosmic dimensions, the Moebius strip extends over distances where the gravitational law is not valid any more. The model calculation of the Moebius strip should better be made by an electric potential, representing the electric or plasma universe. However the electrostatic potential is of type $1/r$ like the gravitational potential. Therefore the result will be qualitatively the same as for the gravitational case we worked out.

3.4 Radial Schrödinger equation

As an example for showing the applicability of the Lagrange mechanism in atomic physics, we solved the radial Schrödinger equation for Hydrogen

$$\frac{d^2\psi}{dr^2} + \frac{2}{r} \frac{d\psi}{dr} - \frac{l(l+1)\psi}{r^2} = \left(\frac{1}{n^2} - \frac{2}{r} \right) \psi \quad (60)$$

numerically. n is the principal quantum number and l is the angular momentum quantum number. Both are related to the classical orbital parameters of ellipses

n	l	a	α	ϵ
1	0	1	0	1
2	0	4	0	1
2	1	4	3	0.7071
3	0	9	0	1
3	1	9	2	0.8819
3	2	9	6	0.5774

Table 1: Parameters of an ellipse in dependence of quantum numbers n, l .

via

$$a = \frac{\hbar n^2}{\alpha_f m c} \quad (61)$$

$$\alpha = \frac{\hbar l (l + 1)}{\alpha_f m c} \quad (62)$$

$$\epsilon = \sqrt{1 - \frac{l (l + 1)}{n^2}} \quad (63)$$

where α_f is the fine structure constant, m the electron mass, a the semi major axis of the orbit, α the half-right latitude and ϵ the eccentricity. Using atomic units, The values of a , α and ϵ have been computed from the quantum numbers as shown in Table 1. Obviously α is zero for all s orbitals, and eccentricity is unity.

Some numerical solutions of Eq. (60) are graphed in Figs. 7 and 8 and compared with the analytically known solutions that we have used in earlier papers. For the calculation, the choice of initial conditions is a certain problem. To have a fair comparison, we used the values for ψ and $d\psi/dr$ at the first r grid point from the analytical solution. Then both the numerical and analytical result lie on each other without visible deviations, giving perfect coincidence. If the initial conditions are taken differently, the curves swing into the correct course within very few grid points.

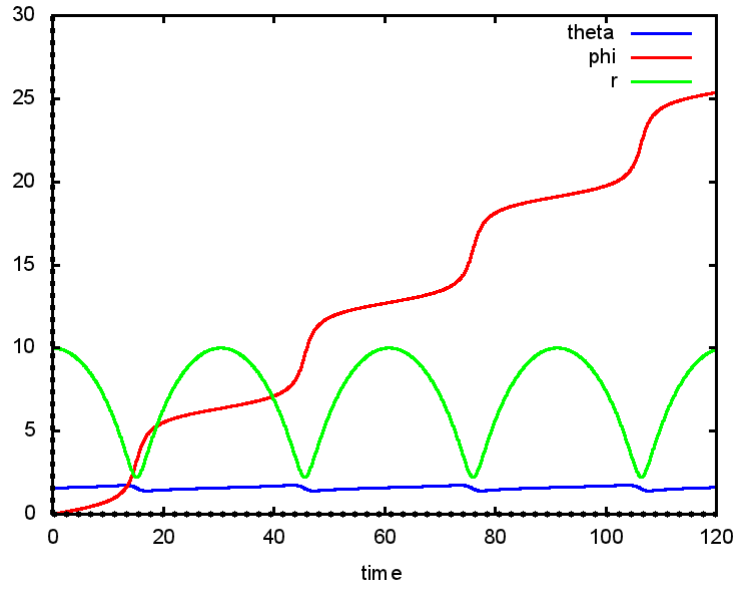


Figure 1: Relativistic trajectories $\theta(t), \phi(t), r(t)$.

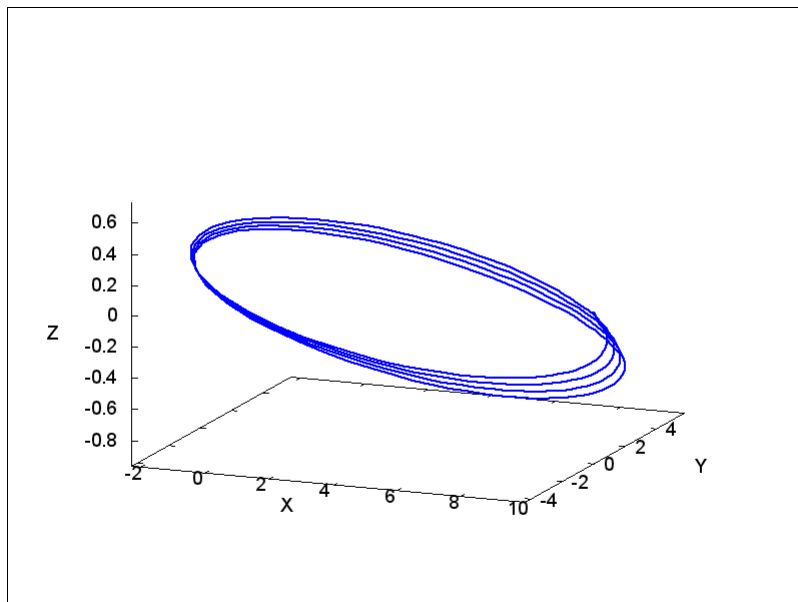


Figure 2: Orbit $r(X, Y, Z)$ of a precessing ellipse.

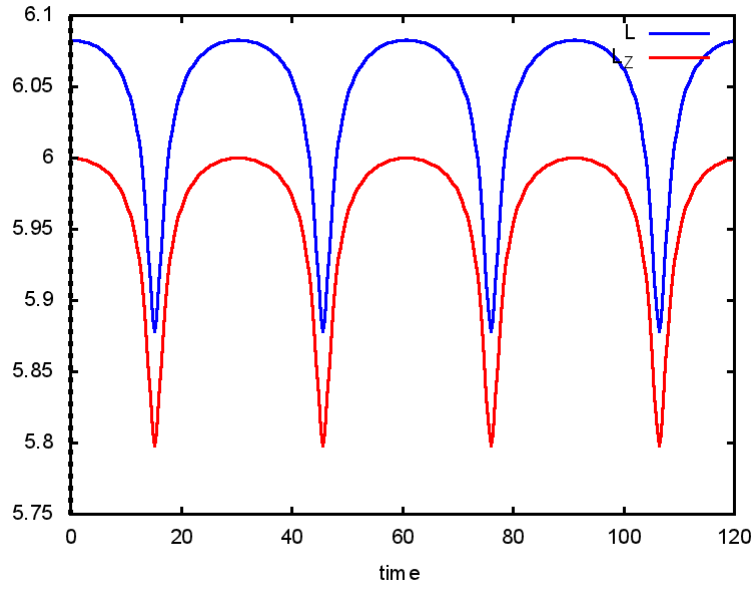


Figure 3: Non-relativistic constants of motion L and L_Z .

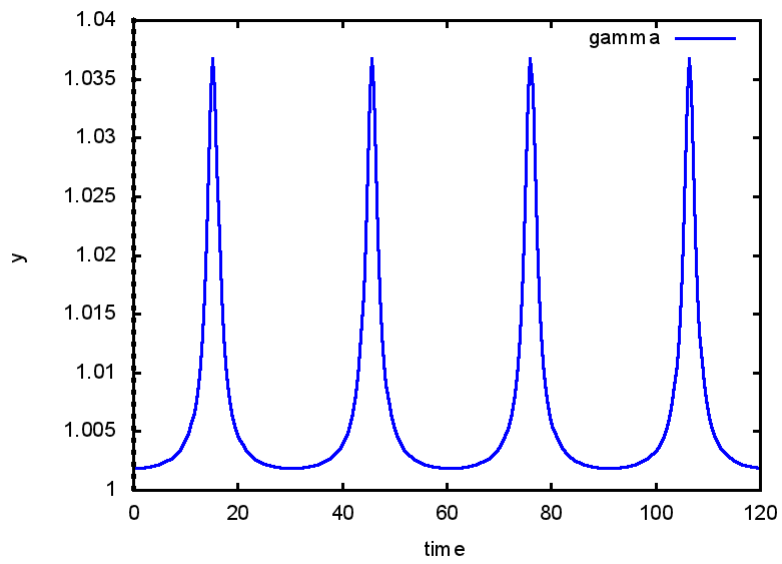


Figure 4: Relativistic γ factor.

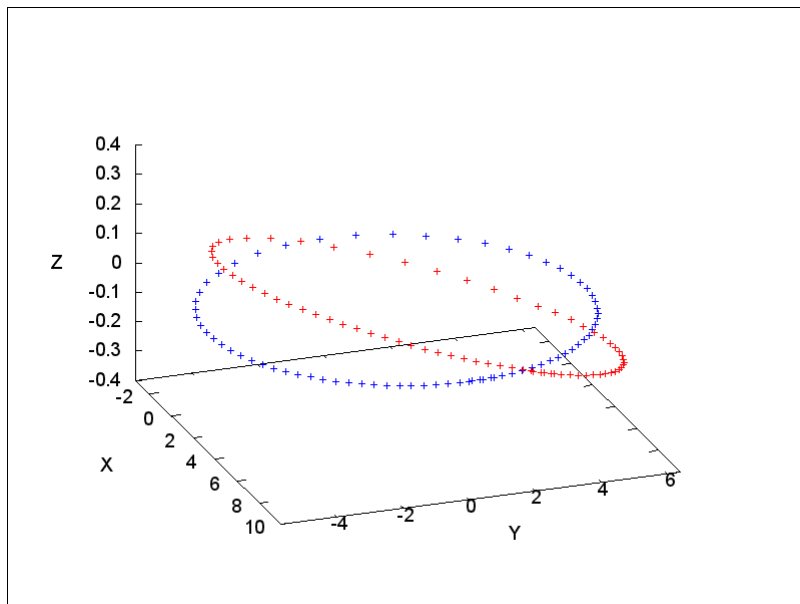


Figure 5: Orbits $r(X, Y, Z)$ of two masses representing a Moebius strip.

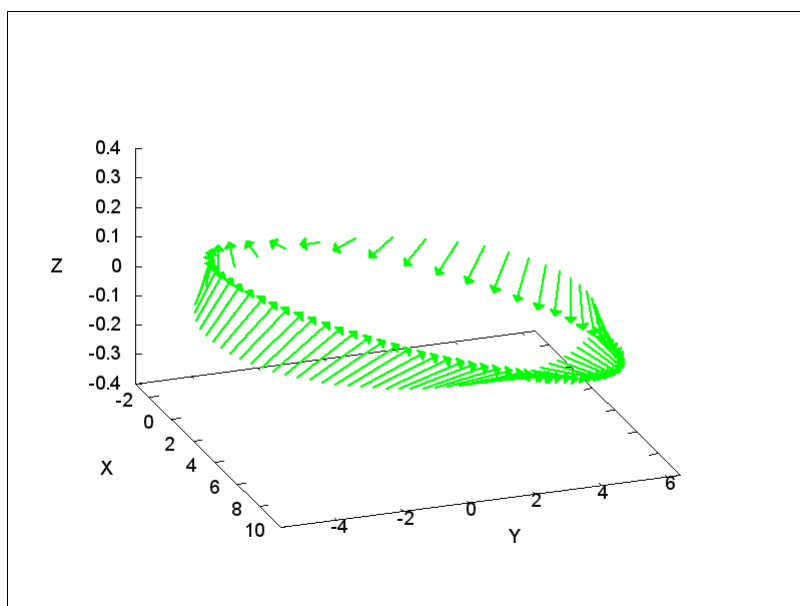


Figure 6: Difference of orbit vectors representing a Moebius strip.

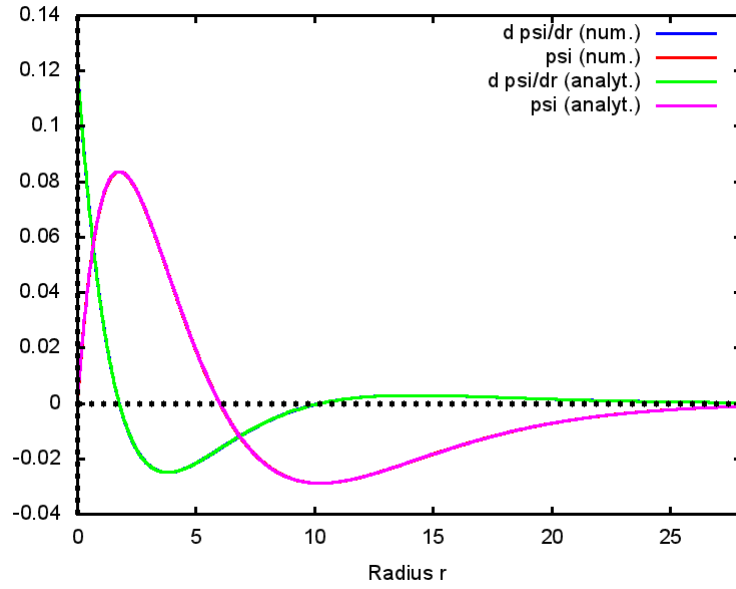


Figure 7: Comparison of Hydrogen orbital 3p (numerical and analytical).

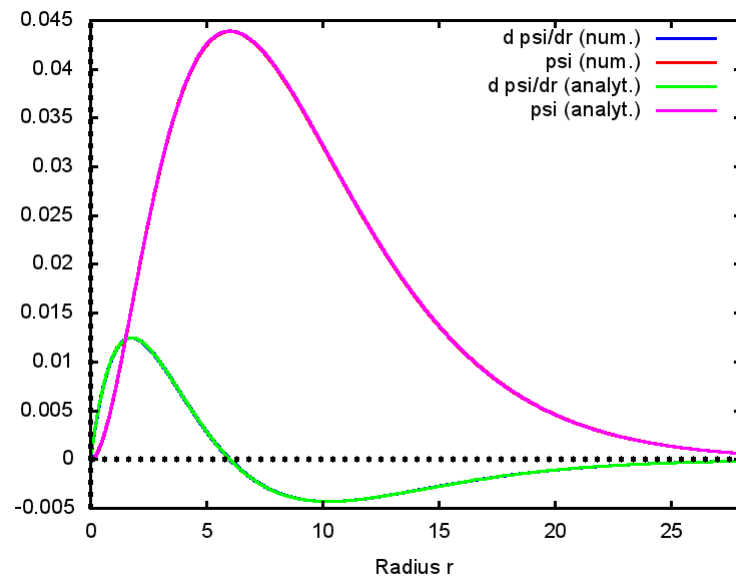


Figure 8: Comparison of Hydrogen orbital 3d (numerical and analytical).

ACKNOWLEDGMENTS

The British Government is thanked for the award of a Civil List Pension, and the staff of AIAS and others for many interesting discussions. Dave Burleigh, CEO of Annexa Inc., is thanked for hardware and software maintenance of the www.aias.us site and feedback programs, Alex Hill is thanked for translation and broadcasting, and Robert Cheshire for broadcasting.

REFERENCES

- {1} M .W. Evans, H. Eckardt, D. W. Lindstrom and S. J. Crothers, “ECE2: The Second Paradigm Shift” (open source UFT366, Spanish Section, and in prep, ePubli Berlin).
- {2} M. W. Evans, H. Eckardt, D. W. Lindstrom and J. S. Crothers, “The Principles of ECE” (open source UFT350, Spanish Section, hardback ePubli 2016, softback New Generation 2016).
- {3} M .W. Evans, S. J. Crothers, H. Eckardt and K. Pendergast, “Criticisms of the Einstein Field Equation” (open source UFT301, hardback Cambridge International (CISP) 2010).
- {4} M .W. Evans, H. Eckardt and D. W. Lindstrom, “Generally Covariant Unified Field Theory” (open source relevant UFT papers, and Abramis, softback in five volumes, 2005 to 2011).
- {5} L. Felker, “The Evans Equations of Unified Field Theory” (open source UFT302 and Spanish Section, Abramis softback 2007).
- {6} H. Eckardt, “The ECE Engineering Model” (open source UFT303, collected equations).
- {7} M. W. Evans, “Definitive Refutations of the Einsteinian General Relativity” (Open source on www.aias.us and CISP 2012, hardback).
- {8} M. W. Evans, “Collected Scientometrics” (Open source UFT307 and New Generation,

2015).

{9} M. W. Evans and L. B. Crowell, "Classical and Quantum Electrodynamics and the B(3) Field" (Open Source, Omnia Opera Section and World Scientific 2001).

{10} M. W. Evans and S. Kielich (Eds.), "Modern Nonlinear Optics" (Wiley Interscience, New York, 1992, 1993, 1997, 2001) in two editions and six volumes.

{11} M. W. Evans and J.-P. Vigi er, "The Enigmatic Photon" (Open source Omnia Opera Section, and Kluwer 1994 to 200 in five volumes each, hardback and softback).

{12} M. W. Evans and A. A. Hasanein, "The Photomagnetron in Quantum Field Theory" (World Scientific, 1994, hardback).